Mechatronic Design of a Fast and Long Range 4 Degrees of Freedom Humanoid Neck

D.M. Brouwer, J. Bennik, J. Leideman, H.M.J.R. Soemers, S. Stramigioli, *Member, IEEE*

***Abstract*— This paper describes the mechatronic design of a humanoid neck. To research human machine interaction, the head and neck combination should be able to approach the human behavior as much as possible. We present a novel humanoid neck concept that is both fast, and has a long range of motion in 4 degrees of freedom (DOFs). This enables the head to track fast objects, and the neck design is suitable for mimicking expressions.**

The humanoid neck features a differential drive design for the lower 2 DOFs resulting in a low moving mass and the ability to use strong actuators. The performance of the neck has been optimized by minimizing backlash in the mechanisms, and by using gravity compensation. Two cameras in the head are used for scanning and interaction with the environment.

I. Introduction

OVER the last couple of years several humanoid heads, including necks with multiple degrees of freedom (DOFs), have been developed. Roughly two different types of necks can be distinguished. The first neck type is a fast moving neck with a short range in just 2 or 3 DOFs. These necks are primarily used for object tracking. Secondly there are less fast moving necks with a larger range of motion in 3 or 4 DOFs. The necks of this type are optimized to express a number of different emotions.

The ASIMO [1] is a humanoid belonging to the first category, which is developed by researchers of Honda. ASIMO is a biped humanoid and is able to interact with humans. The neck of ASIMO has only 2 DOFs. Other examples of necks with 2 DOFs are the GuRoo by University of Queensland [2] and a neck by UC San Diego [3]. The Maveric [4] is a fast 3 DOFs head/neck created by researchers of the University of Southern California.

Examples of necks with a long range of motion are WE-4RII by the the University of Waseda [5], QRIO by Sony [6], the Cog by MIT [7], a neck by the University of Karlsruhe [8], iSHA by Waseda University [9] and the iCub by University of Polytechnics at Madrid [10].

Our goal is to develop a humanoid neck that is both fast enough for tracking objects and flexible enough to mimic human expressions and emotions. The neck will serve as a research platform for human machine interaction, humanoid vision and audio.

The first version of the head and neck is equipped with 2 cameras fixed to the head. The cameras operate with vision software, which is developed at the University of Twente [11]. The control software for the neck movements is also developed at the University of Twente [12].

This paper describes the mechatronic design, development and implementation of the humanoid neck.

II. Specifications

A. Biological data

The human neck is a complex mechanism. The basic control task of a human neck is to keep the head in a ‘neutral’ position whenever possible [13]. The neck consists of 7 vertebrae and the atlas that supports the skull. These vertebrae are usually referred to as C1 through C7 in the existing literature.

Our head and neck design is based on the size of an adult woman. The acceleration, velocity and range specifications of the human head and neck are reported in several studies. However many of the specifications described are contradictorily. For our design, we used a combination of the most challenging specifications found in the literature [14],[15],[16]. Every DOF has an individual range of motion. The velocities and the accelerations in the individual DOFs are the same. The specifications of the human neck we derived from the literature can be found in Table I.

TABLE I
BIOLOGICAL DATA OF THE HUMAN HEAD AND NECK

	Range (°)	Velocity max (°/s)	Acceleration max (°/s^2)
Pitch	-71 to +103	352	3300
Roll	+/- 63.5	352	3300
Yaw	+/- 100	352	3300

Manuscript received September 15, 2008. This work was supported in part by DEMCON advanced mechatronics and in part by the 3TU Center of Excellence on Intelligent Mechatronics systems.

D.M. Brouwer is with the Mechanical Automation and Mechatronics group of the University of Twente, and with DEMCON advanced mechatronics, the Netherlands (corresponding author phone: +31614246303; e-mail: d.m.brouwer@utwente.nl).

J. Bennik is now with Philips Consumer Lifestyle, the Netherlands. (e-mail: janbennik@gmail.com).

J. Leideman is with DEMCON advanced mechatronics, Oldenzaal, the Netherlands (jan.leideman@demcon.nl).

H.M.J.R Soemers is with the Mechanical Automation and Mechatronics group of the University of Twente, and with Philips Applied Technologies, the Netherlands (h.m.j.r.soemers@utwente.nl).

S. Stramigioli, is with the Control Engineering group of the University of Twente, the Netherlands (s.stramigioli@utwente.nl).

A. Humanoid head and neck specifications

A humanoid neck with 4 long range DOFs, as shown in Figure 1, enables the necessary motion for expressions of almost every possible movement of the human head. In this paper we studied the motion of the neck only. To create a long range of motion in the pitch direction, the pitch range as given in Table I is split up into two equal contributions over the lower pitch and the upper pitch.

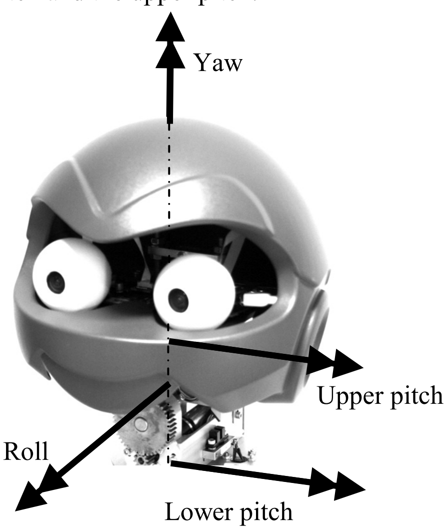

Fig. 1. The 4 DOFs of the humanoid head.

Roughly the control bandwidth (open loop cross-over frequency) is be estimated [17] for the lower yaw and pitch direction. The control bandwidth for the roll and upper pitch movements are less important, because these DOFs are not used for object tracking. A rotation movement angle (h_m) of $\pi/2$ is made using a third order set point input trajectory in a movement time (t_m) of 0.36s. The movement time is based on the maximum acceleration and velocity as specified in Table I. The set point error (e) is the position difference between the set point and the head at the end of the specified movement at $t = t_m$. A reasonable error is estimated at 1.8°, because the much faster tracking of the eyes should not be compromised too much by the performance of the head. The phase lead factor (α_{lead}) of 0.1 is used to minimize the set point error. The required minimum control (ω_c) bandwidth estimated becomes:

$$\omega_c \approx \sqrt[3]{\frac{32h_m}{{t_m}^3}\frac{1/\alpha_{lead}}{e}} / 2\pi = 11Hz \quad (1)$$

The specification for the minimum lowest mechanical natural frequency, can be estimated by multiplying the control bandwidth by a factor 4. The first mechanical resonance frequency should be higher than 44 Hz. It applies to the entire head.

Besides the maximum weight of 3.7 kg of the head and neck itself, the neck should be able to carry an extra payload of 800gr. This extra payload is needed for future peripherals such as audio, skin or the possibility to speak. The weight can be reduced by at least 50% in a future version by optimizing the material usage, optimizing the motor duty cycles and using adequate materials at critical locations.

III. Kinematic concept

The specified 4 DOFs of the neck can be generated by parallel or serial kinematic mechanisms, or combinations. Typically parallel systems result in a low moving mass enabling fast movements [18]. However the range of motion is generally limited. Moreover, parallel mechanisms often rely on prismatic joints requiring linear motors or spindles. The power density of linear motors is small compared to rotary drives and in the case of spindles special back drivable spindles are required to ensure robustness. Therefore a 4 DOFs serial concept is preferred. This complies with an earlier study that concluded that actuating every single DOF in a separate stage with rotational motors was, among the tested neck configurations, the best way to design a humanoid neck [10].

It was not possible to fit the 4 different stages in the neck with sufficiently strong motors due to the size limitations combined with the range, velocity and acceleration specifications. The reason for this is that the stages are stacked on top of each other and the weight and inertia of the upper stages directly lead to higher needed torques for the motors in the lower stages. The performance of the neck can be enhanced by minimizing the weight of the head by shifting the actuators to the body using cables to transfer the energy. However, cables have the disadvantage of increased friction, wear, hysteresis and need pre-tensioning. Therefore, for a relatively fast and accurate system this solution is not preferred.

To avoid the fundamental problem due to stacking of mass in a serial mechanism and the friction problem of a cable driven neck, the motion of the two strongest loaded motors, the yaw and the lower pitch, is generated in parallel by a differential drive. Instead of putting the motors in the neck itself both motors are now placed inside the shoulders. This results in a compact neck with a relative low moving weight. Another advantage is that the motors of the yaw and lower pitch are placed stationary in respect to the neck. This means that larger and stronger motors can be chosen without affecting the performance and the weight of the neck. The roll and the upper pitch are stacked in series on top of the differential drive. The DOFs are shown in Figure 1.

The main disadvantage using a differential drive is that it is more complex than a serial set-up. The differential is built up out of bevel gears requiring alignment with tight tolerances.

IV. Mechatronic design

In this section details of the mechatronic design of the neck for the humanoid will be presented.

A. Differential design and model

The differential consists of two sun wheels, a planet wheel and a differential carrier as shown in Figure 2. The two sun wheels are externally driven gears. The planet wheel is a gear driven by the two sun wheels.

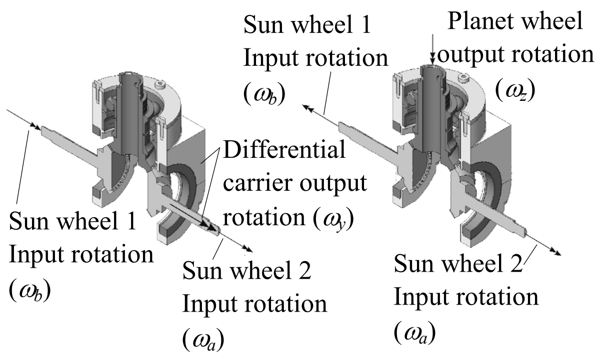

Fig. 2. a) Driving the sun wheels in equal direction causes the differential carrier and therefore the head to pitch, b) When the two sun wheels are rotating in the opposite direction the planet wheel and therefore the head will yaw.

The control of the differential requires a decoupling of the velocities. The generalized velocity, the twist vector $T_1^{0,0}$, expressed in homogeneous coordinates can be decoupled [12] into two separate rotations ω_y and ω_z, shown in Figure 2, with r_s and r_p respectively the radii of the sun and planet wheels:

$$T_1^{0,0} = J\begin{bmatrix}\omega_y \\ \omega_z\end{bmatrix} = \begin{bmatrix}0 & \sin\alpha \\ 1 & 0 \\ 0 & \cos\alpha \\ 0 & 0 \\ 0 & 0 \\ 0 & 0\end{bmatrix}\begin{bmatrix}\frac{1}{2}\left(\omega_a + \omega_b\right) \\ \frac{r_s}{2\,r_p}\left(\omega_a - \omega_b\right)\end{bmatrix} \quad (2)$$

The differential drive, shown in Figure 3, has been implemented using a pair of medium pre-loaded angular contact bearings to define the positions of the sun wheels and the planet wheel. The resulting stiffness in axial, radial and the rotation perpendicular to the shaft rotation direction, is large [19]. A deep groove ball bearing is used to define the rotation of the differential carrier. The high stiffness is a necessity as the first vibration mode frequencies would otherwise have become too low. However, the angular contact bearing differential drive concept comes at the cost of occupying quite some space.

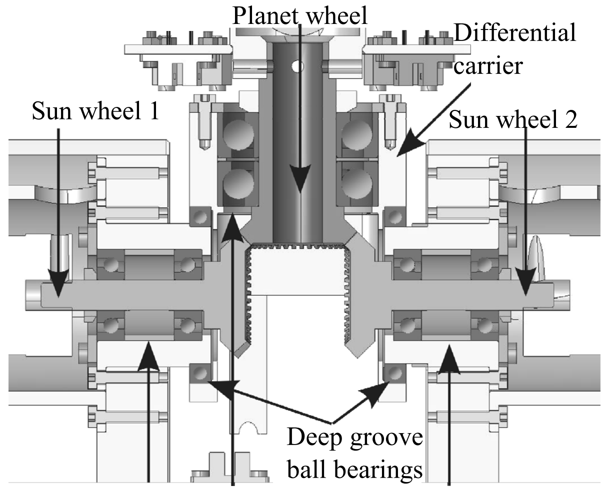

Fig. 3. Differential drive concept with 3 pairs of single row angular contact bearings and a pair of deep groove ball bearings.

B. Bevelgears

The material and the geometry of the gears are chosen and designed in such a way that the gears can handle high continuous and intermitted torques as well as shocks during a long lifetime. The material used for the gears is strong steel: 15CrNi6. The pinions and the gears of the sun wheels and the planet wheel are made out off one piece. This is done to assure a better alignment and better fixation between the sun wheel shaft and the gear during loading by large torques.

Instead of a massive shaft, the shaft of the planet wheel has a hollow tube to combine a high rotational stiffness with low mass. This hollow tube is also used to guide the cables through from the upper part down to the controller boards in the humanoid main body.

C. Mechanical backlash

To make the movements of the neck appear natural and to obtain clear camera images it is necessary to decrease the play in the head as much as possible. Especially backlash, that occurs when the direction of the rotation is inverted, causes discontinuous movements.

To decrease the play in the upper part of the neck a special motor support is designed (Figure 4). This support is a disc in which the motor is placed eccentric. The disc itself is placed centric in the motor housing. By rotating the disc, the distance and the friction between the gear on the motor axle and the second axle can be tuned. Decreasing the distance between the two gears decreases the play but could increase friction. This is an optimization process in which a trade off has to be made between play and friction.

The play in the gearboxes has been reduced by using special low backlash gearboxes manufactured by Gysin. The upper pitch and roll use a Gysin gearbox with less than 0.33° play and the yaw and lower pitch use a Gysin gearbox with less than 0.25° play.

Backlash in the bearings is prevented by preloading them with springs.

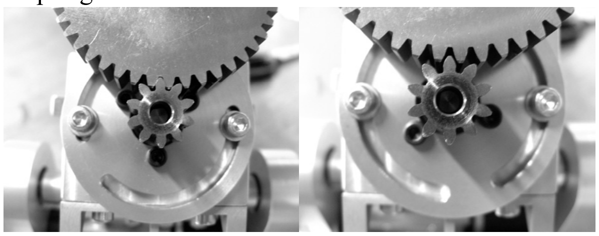

Fig. 4. Adjustable distance between the gear on the motor axle and the gear on the second axle. The situation on the left shows a minimized amount of play but high friction. In the situation on the right the friction is low but the play is large.

D. Safety

To minimize the risk of damage to the head and neck but also to the surroundings as much as possible different safety levels are built in.

The first level is the mechanical safety layer. All DOFs are equipped with mechanical end stops with rubber dampers. These end stops determine the maximal physical possible movement. A second mechanical precaution is integrated in the head plate, which is fixed using a pre-tensioned linear spring (Figure 5). This spring pulls the head plate containing 3 V-grooves onto three balls attached to the top support of the neck. When a collision between the head and an object takes place, the contact between the 3 V-grooves and 3 balls is broken. The impact force on the head is then decoupled from the force on the neck. An electrical switch shuts down the power.

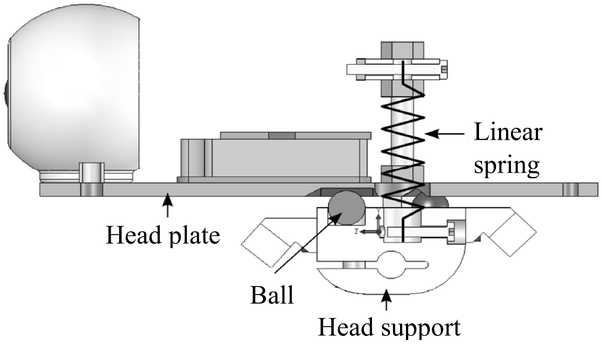

Fig. 5. Collision protection in the head plate and head support. The head support is shown at the upper left. The head plate with the 3 balls positioned in the V-grooves is shown at the upper right.

The second level is an electronic safety layer. Optical switches are placed just before the end stops. They switch off the power if the neck movement is near the end of its range.

In the software a maximum virtual stroke is established. If this maximum stroke is exceeded the power will be shut down. The software also shuts down the power if there is a certain mismatch between the current and the predicted resulting acceleration.

E. Motor and gearbox choice

A dynamic model is developed for the motor-gearbox choices and control purposes using bondgraphs and screw theory [20] by Visser [12]. The design of the head system consists of four rigid bodies (a differential housing, two neck elements and the head) interconnected by joints. The torque and the rotational velocity of the output shaft of the joint motor are transformed into a twist and wrench pair that defines the joint motion.

Each motor and gearbox combination can be optimized using the dynamic model for maximum acceleration in the worst-case scenario with the largest possible inertia. If the specification of the load on the neck is defined with less tolerance in the next stage, the neck can be optimized further.

For the lower pitch and yaw Maxon RE Ø30 60W 24V DC motors are used with a continuous nominal torque of 85mNm. The Roll and upper pitch use Maxon RE max Ø24 11W and A max Ø26 11W DC motors respectively.

F. Gravity compensation

To minimize motor torque and energy loss gravity compensation is applied in the roll and the lower pitch of the neck. The potential energy of the head is balanced with the elastic energy in the pre-loaded springs. The upper pitch and the yaw are not compensated, because the position of the upper pitch and yaw are dependent on the position of the lower pitch and roll. Moreover, the motor load influence by gravity in the upper pitch and yaw direction is relatively small.

The gravity compensation in the roll direction reduces the maximum static motor torque from 0.75 Nm to 0.18 Nm. Two pre-loaded torsion springs are mounted on adjustable bushes. (Figure 6).

The compensation for the lower pitch is realized by two linear springs. Two cables attached to the springs roll over a cam. The gravity compensation in the lower pitch direction reduces the maximum static motor torque from 2.6 Nm to 0.45 Nm. The profile of the cam can be optimized, however, because this neck is used as a research platform and the load on the neck can change, for now a constant radius cam is implemented. At a maximum continuous motor current of 3.4A, the minimum motor torque available for acceleration is increased from 8.4 Nm to 10.6 Nm by the gravity compensation. This seems like a relatively small increase in performance, however with a future version of a heavier head and smaller motors the minimization of torque usage is valuable for downsizing the motors and reducing energy consumption.

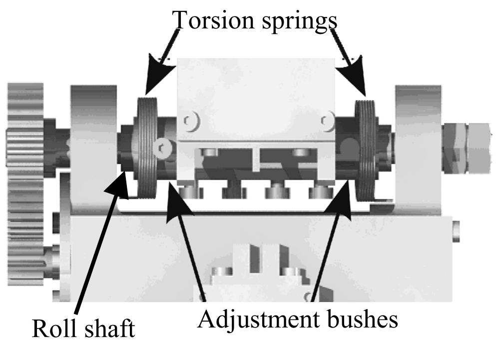

Fig. 6. Gravity compensation for the roll rotation

G. Vibration mode analysis

The dominant compliances in the actuation chain responsible for the lowest vibration mode frequencies of the system are determined, using FEM analysis. The critical components in each DOF are determined. In the roll direction the compliance of the roll shaft, shown in Figure 6, is responsible for a resonance frequency of 31 Hz. The compliance of the sun wheels, shown in Figure 3, determines the lowest natural frequency of 40 Hz in the lower pitch direction. Although these frequencies are smaller than specified, these frequencies are still 3 times larger than the specified bandwidth.

H. Sensors and electronics

To determine the position for each DOF in the neck magnetic encoders are used. The encoders are mounted at the back of the actuators. The lower pith and yaw encoders have 1024 counts per turn. The roll and upper pitch have 1000 and 512 counts per turn respectively. However these encoders do not measure an absolute position, therefore optical switches are used for homing. After the homing procedure the optical switches are used as a safety switch.

For the control of the neck, driving of the motors, reading of the encoders and optical switches two industrial DM3S boards containing an ARM 7 processor are used, which are developed by DEMCON. A DM3S board is able to control three motor drives up to 120 W, 5 A and 30 V. It features 16 digital in and outputs, 12 analogue inputs and 4 analogue outputs and 2 PWM outputs. The controller interfaces are Matlab Simulink based.

For human machine interaction IEEE1394 Fire-I^{TM} cameras are used. The processing of the vision algorithm is done on a mini ITX board. To reduce the amount of wires running through the neck an interconnection board has been implemented.

Figure 7a shows a picture of the first design of the humanoid head and neck. The case below the neck contains the mini ITX computer and 2 DM3S boards. Figure 7b shows a second version of the head with 2 cameras with 3 independent DOFs. Two DOFs are necessary for the rotation of each eye around the vertical axis. A third DOF is necessary for a combined eye motion for looking up and down. The total independent DOFs of the neck combined with eyes amount to 7. The cameras operate with vision software, which is developed at the University of Twente [11]. The control software for the neck movements is also developed at the University of Twente [12].

V. Preliminary results

To validate the specifications of the head, several tests were performed. To test the possible ranges, the angles of the DOFs were measured with activated safety layer using the optical switches. The results are shown in Table II. Figure 8 shows the maximum possible motion ranges of the 4 DOFs during operation. The specified ranges are met except for the roll. The pitch range has been divided slightly different with respect to the specifications. The total size of the head and neck is slightly larger than that of an adult woman.

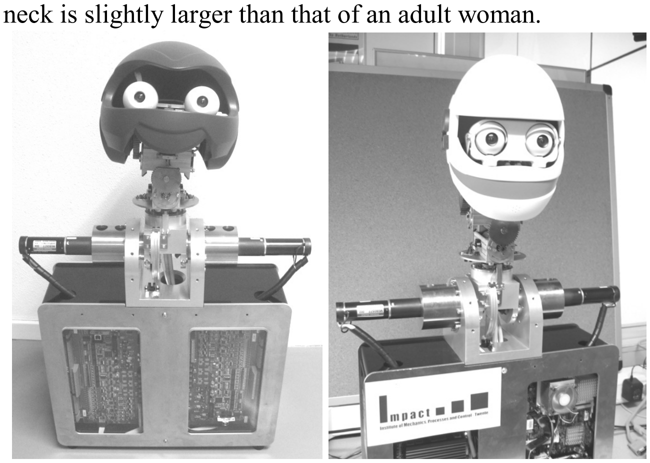

(a) (b)

Fig 7. a) First design of the humanoid head and neck with a mounting case for the boards and a mini ITX computer. b) Second humanoid head design with a 3DOFs independent camera set-up using 20Sim software.

TABLE II
Measured performance results

	Range (°)	Velocity max (°/s)	Acceleration max (°/s^2)
Upper pitch	-35-+41	354	3340
Lower pitch	±36	354	3340
Roll	±102	356	3340
Yaw	±49	356	3340

To verify if the specified velocities and accelerations are met, a known sinusoidal movement was set as input on every DOF. The motor encoders were used to measure the velocities and accelerations. The frequency of the motion has been increased until the specifications were met. As we did not want to test destructively the acceleration was not increased further.

VI. Conclusions

A mechatronic design of a fast and long range 4DOFs neck for a humanoid is presented. The design comprises a differential drive which reduces moving mass. This helps to combine a fast tracking motion with the required long range of motion. The implemented differential drive concept results in high structural stiffness, which is required for the minimum vibration mode frequency specifications. Several methods have been shown to decrease mechanical backlash in the mechanism. Gravity compensation is applied in 2 DOFs, in order to reduce the motor size, and decrease energy loss.

Safety precautions are implemented at several levels in the mechanics, electronics and software of the head.

The maximum velocities and accelerations have been measured and meet the specifications. The range of motion in the impendent DOFs is also met except for the roll direction. The total size of the head and neck is slightly larger than that of an adult woman. The head and neck provide a good research platform for the future.

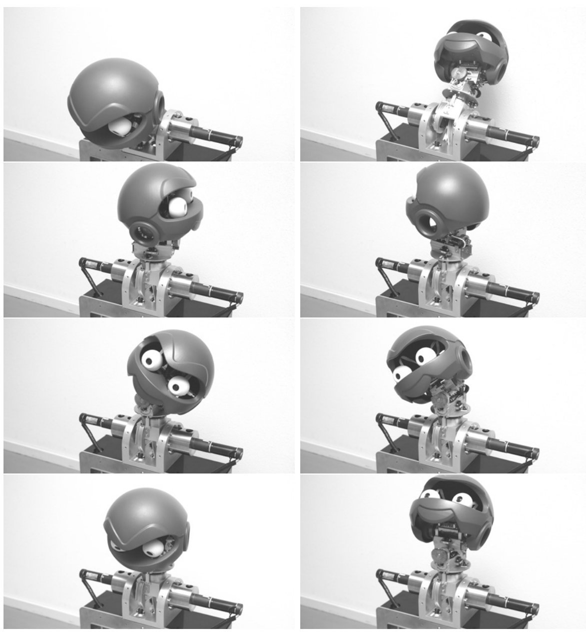

Fig. 8. The independent DOFs in a top to bottom order: lower pitch, yaw, roll and upper pitch.

VII. Discussion

The weight of the current neck can be reduced by at least 50% by optimizing the material usage and optimizing the motor duty cycles.

By using end reductions larger than 1:5 between all gearboxes and the DOFs of the head, in combination with the play reduction motor supports of Figure 4, the play of the head can be minimized using standard gearboxes.

Acknowledgements

The authors would like to thank Ludo Visser, Rob Reilink and Windel Bouwman for helping with the motion control and vision algorithm. We would like to thank Dennis Schipper for supporting the project mentally and financially.

References

[1] M. Hirose, Y. Haikawa, T. Takenaka, and K. Hirai, "Development of humanoid robot ASIMO", in *Proc. IEEE/RSJ Int. Conf. on Intelligent Robots and Systems*, Workshop 2, Hawaii, USA, 2001.

[2] G. Wyeth, D. Kee, M. Wagstaff, N. Brewer, J. Stirzaker, T. Cartwright, and B. Bebel, "Design of an autonomous humanoid robot", in *Proc. of the Australian Conference on Robotics and Automation (ACRA 2001)*, Melbourne, August-September 2001.

[3] H. Kim, G. Cork, G. Burton, E. Murphy-Chutorian, and J. Triesch, "Design of an anthropomorphic robot head for studying autonomous development and learning", *Proc. of the IEEE 2004 Int. Conference on Robotics and Automation*, New Orleans, LA, April-May 2004.

[4] Maveric, http://www-humanoids.usc.edu/HH_summary.html

[5] K. Itoh et al, "Various emotional expressions with emotion expression humanoid robot WE-4RII Robotics and Automation", in Proc. *IEEE Technical Exhibition Based Conference on Robotics and Automation*, TExCRA apos;04.,18-19 Nov. 2004, Page(s): 35 – 36

[6] L.Geppert. Qrio, "the robot that could", *IEEE Spectrum*, 41(5):34-37, May 2004.

[7] A. Brooks, C. Breazeal, M. Marjanovic, B. Scassellati, and M. M. Williamson, *The cog project: Building a humanoid robot, Lecture Notes in Artificial Intelligence, Computation for Metaphors, Analogy and Agents*, 1562(1), 1998.

[8] A. Albers, S. Brudniok, and W. Burger, "The mechanics of a humanoid", In *Proc. of Humanoids 2003*, Karlsruhe, Germany, 2003.

[9] K. Suzuki and S. Hashimoto, "Harmonized human-machine environment for humanoid robot", In IEEE, editor, *Proceedings of the 2001 IEEE-RAS International Conference on Humanoid Robots*, Japan, 2001.

[10] R. Beira, M. Lopes, M. Praca, J. Santos-Victor, A. Bernardino, G. Metta, F. Becchi, and R. Saltaren, "Design of the robot-cub (icub) head," in *Proceedings IEEE International Conference on Robotics and Automation*, 2006.

[11] R. Reilink, *"Realtime Stereo Vision Processing for a Humanoid"*, MSc-Report 019CE2008, University of Twente, June 2008S.

[12] L.C. Visser, *"Motion Control of a Humanoid Head"*, MSc-Report 016CE2008, Control Laboratory, University of Twente, June 2008.

[13] K. Berns, C. Hillenbrand and K. Mianowski, "The Mechatonic Design of a Human-like Robot Head", *Courses and lectures-international centre for mechanical sciences*, Springer-Verlag, 2006, Nb 487, p263-270.

[14] D. Wagner, J.A. Birt, M. Snyder and J.P. Duncanson, "Human factors design guide" , Internal report of FAA William J.Hughes Technical Center, 1996.

[15] W.H. Zangemeister and L. Stark, "Active head rotations and eye-head coordination", Annals of the *New York Academy of Science*, 374:540-59, 1981.

[16] J. Panero and M. Zelnik, *Human Dimensions and Interior Space*, Watson-Guptill Pubs, 1979.

[17] H.M.J.R. Soemers, *Mechatronc Design of Motion Systems,* Lecture notes, University of Twente, 2006

[18] L.W. Tsai, *Robot Analysis: the mechanics of serial and parallel manipulators*, Wiley Interscience. John Wiley and Sons, 1999.

[19] *Radial and axial stiffnesses of ball bearings*, Philips, Internal report, 2002.

[20] S. Stramigioli and H. Bruyninckx, "Geometry and screw theory for robotics," in *Proceedings IEEE International Conference on Robotics and Automation*, 2001.